NANO LETTERS

Letter

pubs.acs.org/NanoLett

Strain-Engineering of Band Gaps in Piezoelectric Boron Nitride Nanoribbons

Jingshan Qi,[†,‡] Xiaofeng Qian,*[,§] Liang Qi,[§,∥] Ji Feng,[⊥] Daning Shi,[‡] and Ju Li*[,§,∥]

[†]College of Physics and Electronic Engineering, Jiangsu Normal University, Xuzhou 221116, China

[‡]Department of Applied Physics, Nanjing University of Aeronautics and Astronautics, Nanjing 210016, China

[§]Department of Nuclear Science and Engineering and Department of Materials Science and Engineering, Massachusetts Institute of Technology, Cambridge, Massachusetts 02139, United States

[∥]State Key Laboratory for Mechanical Behavior of Materials and Frontier Institute of Science and Technology, Xi'an Jiaotong University, Xi'an, 710049, China

[⊥]International Center for Quantum Materials, School of Physics, Peking University, Beijing 100871, China

Supporting Information

ABSTRACT: Two-dimensional atomic sheets such as graphene and boron nitride monolayers represent a new class of nanostructured materials for a variety of applications. However, the intrinsic electronic structure of graphene and h-BN atomic sheets limits their direct application in electronic devices. By first-principles density functional theory calculations we demonstrate that band gap of zigzag BN nanoribbons can be significantly tuned under uniaxial tensile strain. The unexpected sensitivity of band gap results from reduced orbital hybridization upon elastic strain. Furthermore, sizable dipole moment and piezoelectric effect are found in these ribbons owing to structural asymmetry and hydrogen passivation. This will offer new opportunities to optimize two-dimensional nanoribbons for applications such as electronic, piezoelectric, photovoltaic, and opto-electronic devices.

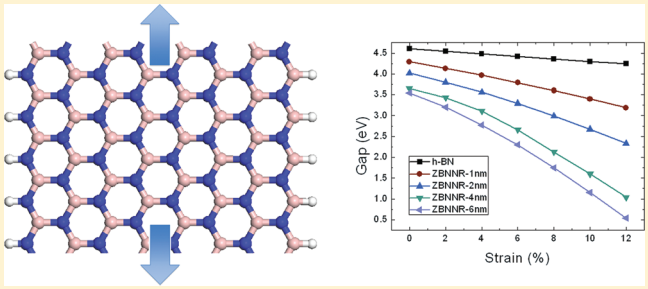

KEYWORDS: *Elastic strain engineering, ESE, nanoribbon, piezoelectricity*

Two-dimensional materials, such as graphene[1−5] and hexagonal boron nitride (h-BN) monolayers,[6] are attractive for their fascinating physics and potential applications in next-generation electronics. Single atomic layer thickness makes it possible to fabricate devices with channels that are extremely thin. This will allow field-effect transistors (FETs) to be scaled to shorter channel heights and higher speeds without encountering the adverse short-channel effects that restrict the performance of existing devices.[1] However, we must overcome a few fundamental difficulties. First, FETs with large-area graphene channels cannot be switched off because it is a semimetal with zero band gap. To give a large on−off ratio in the conductance, required for electronic logic, it is necessary for them to possess a significant electronic energy gap E_g. The ballpark value for E_g should be around that of silicon, 1.1 eV. For this purpose, energy gaps were opened by cutting graphene into ultranarrow nanoribbons (GNRs).[7,8] However, their band gaps depend strongly on the types of the edges and widths[7] of GNRs and therefore encounter serious issues with fabrication because of the small widths (less than 5 nm) required for getting a big enough band gap. On the other hand, monolayer h-BN and h-BN nanoribbons (BNNRs) with edges passivated by hydrogen are all wide-gap semiconductors,[9] making them unsuitable as FET channels at room temperature. Recently, another strategy[10] was experimentally demonstrated by hybridizing h-BN and graphene (h-BNC) domains. However, their random distribution may introduce difficulties in fabricating nanoscale h-BNC films with uniform electronic properties. It would, therefore, be highly desirable to have capabilities to continuously control the band gap of two-dimensional materials for building future electronic and optoelectronic devices.

One promising route toward the continuously tunable band gap is elastic strain engineering (ESE),[11] which allows one to control the electronic properties of materials by simply applying an elastic strain. Although large elastic strain rarely exists in bulk materials since they are easily relaxed by dislocation plasticity or fracture, plasticity and fracture are greatly delayed in nanostructures ("smaller is stronger"), allowing for a much larger dynamical range of applying elastic strain reversibly.[11] For example, experimentally measured breaking strength of graphene monolayer was as high as 13% of ideal strength, while that of bulk graphite seldom reaches 0.1%.[12,13] Unfortunately, uniaxial elastic strain will not open an energy gap for infinite graphene within 20% strain.[14−17] In the case of zigzag GNRs,

Received: October 11, 2011
Revised: February 3, 2012
Published: February 24, 2012

uniaxial strain also has little influence on the band structure.[18−22] Although the energy gaps of armchair GNRs are predicted to change as a function of the applied uniaxial strain, the tunable window of the energy gap becomes narrower when the width of ribbon increases.[18−22]

In this Letter, we demonstrate by first-principles calculations that band gap of zigzag BNNRs (ZBNNRs) can be significantly tuned by applying a uniaxial strain. We find that the wider ZBNNRs are, the more easily the band gaps can be tuned under the same strain, demonstrating distinctly different physics from GNRs. Moreover, ZBNNRs possess sizable dipole moment, and more importantly the magnitude and direction of the dipole moment change substantially under elastic strain, resulting in a polarization switch at finite strain. These findings imply their potential applications in electronic, piezoelectric, photovoltaic, and opto-electronic devices. We will also elucidate below the underlying mechanism of strain- and width-dependent band gap and polarization.

First-principles density-functional theory (DFT) calculations were performed in a supercell configuration using the Vienna ab initio simulation package (VASP).[23] We employed projector augmented-wave (PAW) method,[24] the local-density approximation (LDA)[25] of exchange-correlation functionals, an energy cutoff of 400 eV for the plane-wave basis, and 50 Monkhorst-Pack *k*-points along the nanoribbon axis. Geometry optimizations were performed with a criterion of the maximum residual force less than 0.02 eV/Å without any symmetry constraints. The supercell was adjusted to maintain a sufficiently large separation between adjacent nanoribbons (>15 Å from surface to surface). A representative atomic structure of 2 nm wide ZBNNR is shown in Figure 1, which has two distinct edges

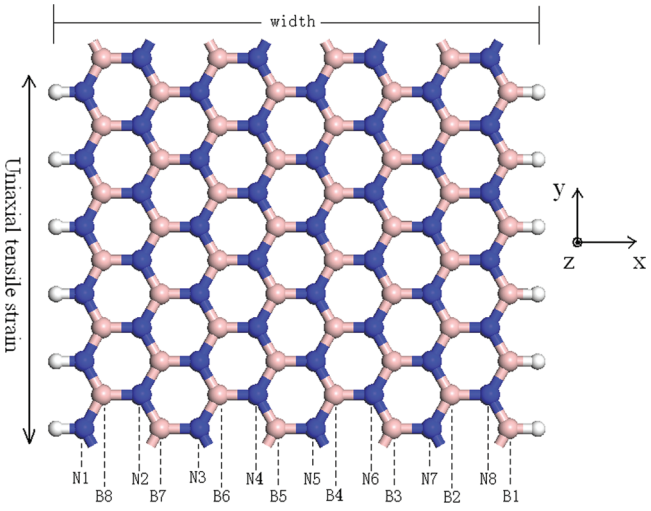

Figure 1. Atomic structure of 2 nm wide ZBNNR. Each B or N atom row along nanoribbon width direction is labeled.

terminated by N and B atoms, called N-edge and B-edge, respectively, with all edge atoms further passivated by H atoms. As presented in Supporting Information, the band gap and polarization using the generalized gradient approximation of exchange-correlation functionals are almost the same as the LDA results except for a small constant shift. It is known that DFT with LDA in general underestimates the band gaps of materials and more accurate estimation of band gaps requires a quasiparticle approach.[26] Nevertheless, the general trends of width-dependent and strain-dependent band gap and piezoelectricity described here are unlikely to change.

The width and strain dependence of energy gap are presented in Figure 2 for monolayer h-BN and ZBNNRs

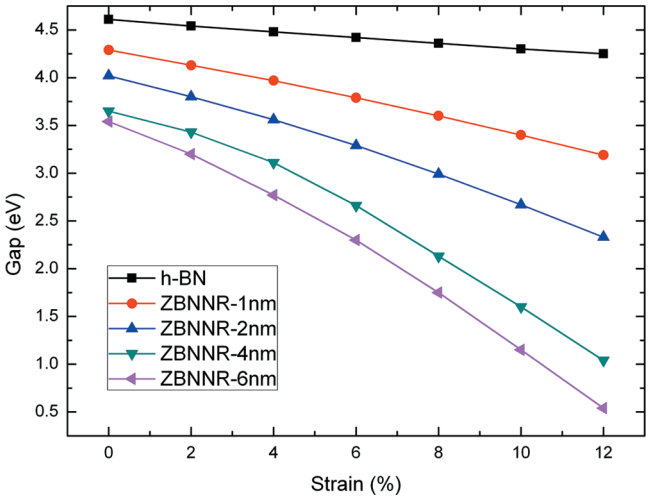

Figure 2. The variation in band gaps of monolayer h-BN and ZBNNRs with different widths from 1 to 6 nm under the uniaxial tensile strain.

with uniaxial tensile strain applied along the zigzag direction. We can see that band gap of monolayer h-BN has slight changes, while band gaps of ZBNNRs decrease significantly with increased tensile strain. The wider the ribbon is, the more rapidly the gap decreases. For example, 10% elastic strain reduces the band gap of 6 nm wide ZBNNR from about 3.5 to 1.0 eV. A previous study has indicated that the maximum elastic strain which BNNRs can take is over 20%.[27] Thus, ESE of ZBNNRs appears to be a promising approach to reduce the large band gap of h-BN down to the silicon range. The origin of the above width and strain dependence of the energy gaps can be understood from electronic band structures and wave functions shown in Figure 3. Clearly, ZBNNRs are indirect

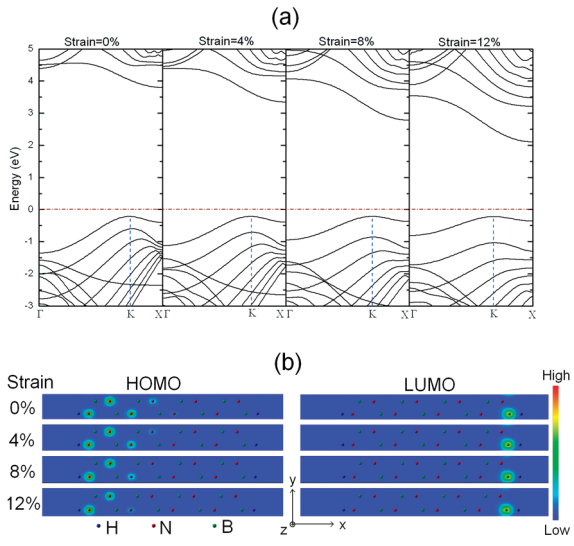

Figure 3. (a) Band structures of 2 nm wide ZBNNRs under different uniaxial tensile strains. (b) Charge densities of HOMO and LUMO under the different uniaxial strains.

dx.doi.org/10.1021/nl2035749 | *Nano Lett.* 2012, 12, 1224−1228

band gap semiconductors with the highest occupied molecular orbital (HOMO) located at K point and the lowest unoccupied molecular orbital (LUMO) located at X point. Charge densities of HOMO and LUMO states under the different uniaxial strains are shown in Figure 3b. We can see that HOMO corresponds to an edge state decaying inward from the N-edge with $2p_z$ character on nitrogen atoms, while the LUMO is an edge state localized at the B-edge with $2p_z$ character on boron atoms. These are in agreement with previous results.[28−31] As the strain increases, HOMO becomes more localized toward the N-edge, while LUMO does not change much. These localized quasi-one-dimensional edge states fundamentally differ from the delocalized two-dimensional states in bulk h-BN. Thus, as indicated in Figure 2, the band gap of ZBNNRs will not converge to that of h-BN even if the width of ZBNNRs goes to infinity. The width dependence of the band gap results from quasi-one-dimensional nature of the localized edge states, instead of quantum confinement of the bulk states (the conventional quantum kinetic energy argument). A detailed explanation of the width-dependent band gap is included in Supporting Information. When uniaxial tensile strain is applied along the ribbon axis of ZBNNRs, the B−N bond along the ribbon axis becomes longer, thus the hybridization of $2p_z$ orbitals of N and B atoms on the edges reduces, resulting in a smaller band gap. Because of the spatial separation of the edge states, electrons and holes are localized on the opposite edges of the ZBNNRs, which may give rise to interesting transport, thermoelectric, and optical properties.

The structural asymmetry of ZBNNRs not only leads to two asymmetric edge states but also introduces spontaneous polarization with a residual dipole moment along the width axis. Here we calculate the dipole moment density using the following equation, $P = (1/c)\int_{\text{supercell}} x\rho(x,y,z)\mathrm{d}x\,\mathrm{d}y\,\mathrm{d}z$, where $\rho(x,y,z)$ is the total charge density including negative valence electronic charge and positive ionic charge, w is the ribbon width, and c is the length of super cell (see Figure 1). As shown in Figure 4, the direction of dipole moment density is negative

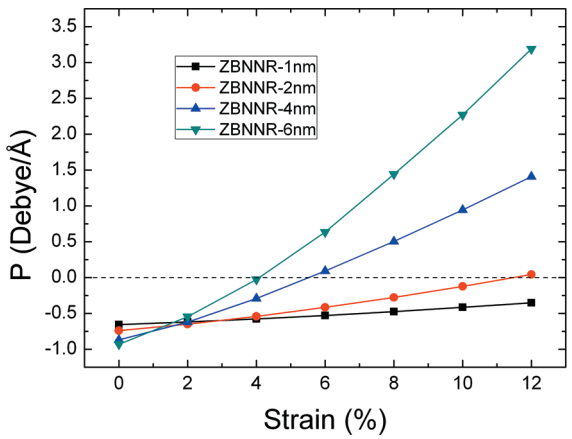

Figure 4. The variation of the dipole moment density of ZBNNRs with uniaxial tensile strain.

under zero strain. With increasing strain, dipole moment density increases gradually, indicating electron transfer toward N-edge. The direction of the dipole moment flips when the strain is above a critical value. For example, the critical strain of 6 nm wide ZBNNR is about 4% only, which is a reasonable critical elastic strain in the ultrastrength regime[11] (but much smaller than the ideal elastic strain limit of >20%[27]). Therefore, ZBNNRs act just like a giant polar molecule with a permanent dipole moment. The long aspect ratio of nanoribbon means we can mechanically "grab" and stretch this molecule. Importantly, the magnitude and direction of dipole moment density of giant polar molecules can be significantly tuned by stretching them along the ribbon axis. We find that this polarization switch is attributed to the strain-induced electron transfer toward the N-edge, and more details are presented in Supporting Information. ZBNNRs, therefore, combine the advantages of semiconducting properties and piezoelectric properties, which hold promising potential in nanoelectro-mechanical devices, such as piezoelectric sensors and piezoelectric nanogenerators.

However, the negative spontaneous polarization of ZBNNRs under zero strain may sound counterintuitive. In fact, N has a larger Pauling electronegativity[32,33] than B, $\chi(\mathrm{N}) = 3.04 > \chi(\mathrm{B}) = 2.04$, hence in principle it will take electron from B. Consequently, the N-edge and the B-edge seemingly should be negatively and positively charged, respectively, resulting in a positive dipole moment. Thus, the negative transverse spontaneous polarization in Figure 4 must be related to the presence of the hydrogen passivation at two edges. Indeed, our additional calculations yield positive dipole moments if ZBNNRs are "naked", that is, without any hydrogen passivation. However, when hydrogen is attached to the left of the N-edge, it adds a strong negative contribution to P, as $\chi(\mathrm{H}) = 2.20 < \chi(\mathrm{N}) = 3.04$ and N would take electron from H, so the H−N bond would be strongly negatively polarized. Whereas, on the other side of the ribbon when a column of H is added to the right of the B-edge, because $\chi(\mathrm{H}) = 2.20 > \chi(\mathrm{B}) = 2.04$, H can actually take electron from B, and the B−H bond should also be negatively polarized. Therefore, the two negative polarization contributions overwhelm the originally positive polarization of "naked" ZBNNR. In effect, the positive net charge of the N-edge should be attributed to H of the H−N bond, while the negative net charge of the B-edge should be attributed to the H of the B−H bond. This charge asymmetry between left and right is a consequence (albeit a bit subtle) of the structural asymmetry of ZBNNR, giving rise to the above spontaneous polarization at zero elastic strain and a permanent transverse dipole moment density, which is different from BN nanotubes.[34]

For device applications, effective mass of carriers is also important. It is defined as $m^* = \hbar^2[d^2E(k)/dk^2]^{-1}$, where $E(k)$ is the energy band, k is the coordinate vector in reciprocal space, and $\hbar$ is the reduced Planck constant. The effective masses of electron and hole are shown in Figure 5 in the units of m_e (m_e is the free electron mass). The effective electron and hole masses converge rapidly with increasing widths, indicating weak width dependence for wide nanoribbons. However, for ZBNNRs with the same width the effective hole mass increases significantly (by 50% from $0.85m_e$ to $1.30m_e$ with 12% strain) and the effective electron mass decreases substantially (by 25% from $1.6m_e$ to $1.2m_e$ with 12% strain). Over a certain large strain (about 11%) the effective mass of the hole is larger than the effective mass of the electron. The large strain-dependent variation of effective mass demonstrates the possibility of tuning carrier mobilities of doped ZBNNRs by applying ESE.

Lastly, we remark on the physical significance of the band gap. For photovoltaic applications, not only the band gap itself needs to be tuned (Shockley−Queisser analysis)[35] for controlling the optimal light spectrum to absorb, but also the oscillator strength needs to be tuned for controlling the

dx.doi.org/10.1021/nl2035749 | Nano Lett. 2012, 12, 1224−1228

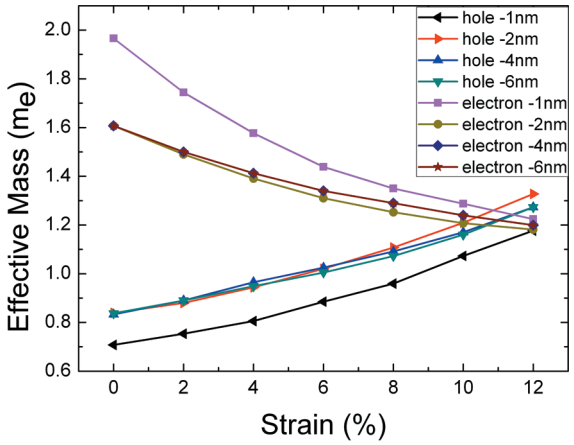

Figure 5. The effective masses (in units of the free electron mass m_e) of electron and hole for ZBNNRs with different widths under different uniaxial tensile strains.

absorption coefficient. The direct transition between the spatially separated HOMO and LUMO is optically weak, because wave function overlap between edge-localized HOMO and LUMO decays exponentially with the ribbon width. However, optical absorption spectrum of ZBNNRs involves all possible optical excitations by promoting electrons from every valence band to every conduction band. Our additional calculations confirm that there indeed exist high-lying valence states spatially close to LUMO and low-lying conduction states spatially close to HOMO, indicating the transition between them are optically allowed. Furthermore, as shown in Figure 3a, the energy level between these optically allowed excitations also reduces upon elastic strain. This means the optical absorption spectrum of ZBNNRs is also strain dependent, implying that elastic strain could possibly be utilized to optimize the optical absorption spectra of ZBNNRs for photovoltaic applications. However, for FET applications the wave function overlap issue above is not as important; the band gap should still be the main consideration because thermal excitation instead of optical excitation is utilized in controlling the carrier concentration. Indeed, electric field has been used in bilayer graphene[36] to generate a continuously tunable band gap up to 0.25 eV, and FET device based on this perpendicular electric field has been demonstrated.[37] The main difference with our case is that the electric field there is externally applied, whereas it is internally generated here via the static dipole and piezoelectric effect.

In conclusion, by first-principles calculation we show that the band gaps of ZBNNRs can be tuned significantly by applying a uniaxial tensile strain within the elastic range and this special property roots in the reduction of orbital hybridization along the ribbon axis upon elastic strain. Furthermore, we find that under the same strain, the wider the nanoribbon, the smaller the gap, which is a result of the localized edge states instead of quantum confinement of the bulk states (the conventional quantum kinetic energy argument). The above findings provide us a practical method to tune their electronic and optical properties with elastic strain engineering. In addition, due to structural asymmetry and hydrogen passivation ZBNNRs possess a permanent transverse dipole moment, like a giant polar molecule. The magnitude and direction of the dipole moment can be tuned significantly by stretching this "molecule", with a significant effect on the band gap and carrier mobility. The phenomena predicted here should be general and may open new avenues of optimizing two-dimensional semiconducting and insulating nanoribbons for electronic, piezoelectric, photovoltaic, and opto-electronic applications.

■ ASSOCIATED CONTENT

Supporting Information

Additional information and figures. This material is available free of charge via the Internet at http://pubs.acs.org.

■ AUTHOR INFORMATION

Corresponding Author

*E-mail: (X.Q) qianxf@mit.edu; (J.L.) liju@mit.edu.

Notes

The authors declare no competing financial interest.

■ ACKNOWLEDGMENTS

This work was supported by 973 Program of China (2010CB631003, 2012CB619402), NSF DMR-1120901 and AFOSR FA9550-08-1-0325. J.Q. also thanks the support by PAPD and NSFJS No. BK2010499.

■ REFERENCES

(1) Schwierz, F. *Nat. Nanotechnol.* **2010**, *5*, 487−496.
(2) Novoselov, K. S.; Geim, A. K.; Morozov, S. V.; Jiang, D.; Zhang, Y.; Dubonos, S. V.; Grigorieva, I. V.; Firsov, A. A. *Science* **2004**, *306*, 666−669.
(3) Geim, A. K.; Novoselov, K. S. *Nat. Mater.* **2007**, *6*, 183−191.
(4) Geim, A. K. *Science* **2009**, *324*, 1530−1534.
(5) Castro Neto, A. H.; Guinea, F.; Peres, N. M. R.; Novoselov, K. S.; Geim, A. K. *Rev. Mod. Phys.* **2009**, *81*, 109−162.
(6) Novoselov, K. S.; Jiang, D.; Schedin, F.; Booth, T. J.; Khotkevich, V. V.; Morozov, S. V.; Geim, A. K. *Proc. Natl. Acad. Sci. U.S.A.* **2005**, *102*, 10451−10453.
(7) Son, Y.-W.; Cohen, M. L.; Louie, S. G. *Phys. Rev. Lett.* **2006**, *97*, 216803.
(8) Barone, V.; Hod, O.; Scuseria, G. E. *Nano Lett.* **2006**, *6*, 2748−2754.
(9) Topsakal, M.; Akturk, E.; Ciraci, S. *Phys. Rev. B* **2009**, *79*, 115442.
(10) Ci, L.; Song, L.; Jin, C. H.; Jariwala, D.; Wu, D. X.; Li, Y. J.; Srivastava, A.; Wang, Z. F.; Storr, K.; Balicas, L.; Liu, F.; Ajayan, P. M. *Nat. Mater.* **2010**, *9*, 430−435.
(11) Zhu, T.; Li, J. *Prog. Mater. Sci.* **2010**, *55*, 710−757.
(12) Liu, F.; Ming, P.; Li, J. *Phys. Rev. B* **2007**, *76*, 064120.
(13) Lee, C.; Wei, X. D.; Kysar, J. W.; Hone, J. *Science* **2008**, *321*, 385−388.
(14) Pellegrino, F. M. D.; Angilella, G. G. N.; Pucci, R. *Phys. Rev. B* **2010**, *81*, 035411.
(15) Choi, S.-M.; Jhi, S.-H.; Son, Y.-W. *Phys. Rev. B* **2010**, *81*, 081407.
(16) Mohr, M.; Papagelis, K.; Maultzsch, J.; Thomsen, C. *Phys. Rev. B* **2009**, *80*, 205410.
(17) Pereira, V. M.; Castro Neto, A. H.; Peres, N. M. R. *Phys. Rev. B* **2009**, *80*, 045401.
(18) Chang, C. P.; Wu, B. R.; Chen, R. B.; Lin, M. F. *J. Appl. Phys.* **2007**, *101*, 063506.
(19) Sun, L.; Li, Q. X.; Ren, H.; Su, H. B.; Shi, Q. W.; Yang, J. L. *J. Chem. Phys.* **2008**, *129*, 074704.
(20) Rasuli, R.; Rafii-Tabar, H.; zad, A. I. *Phys. Rev. B* **2010**, *81*, 125409.
(21) Lu, Y.; Guo, J. *Nano Res.* **2010**, *3*, 189−199.
(22) Li, Y.; Jiang, X.; Liu, Z.; Liu, Z. *Nano Res.* **2010**, *3*, 545−556.
(23) Kresse, G.; Furthmuller, J. *Comput. Mater. Sci.* **1996**, *6*, 15.
(24) Kresse, G.; Joubert, D. *Phys. Rev. B* **1999**, *59*, 1758−1775.
(25) Perdew, J. P.; Zunger, A. *Phys. Rev. B* **1981**, *23*, 5048−5079.
(26) Hybertsen, M. S.; Louie, S. G. *Phys. Rev. B* **1986**, *34*, 5390.
(27) Topsakal, M.; Ciraci, S. *Phys. Rev. B* **2010**, *81*, 024107.

(28) Nakamura, J.; Nitta, T.; Natori, A. *Phys. Rev. B* **2005**, *72*, 205429.
(29) Park, C. H.; Louie, S. G. *Nano Lett.* **2008**, *8*, 2200−2203.
(30) Zhang, Z. H.; Guo, W. L. *Phys. Rev. B* **2008**, *77*, 075403.
(31) Zheng, F. W.; Liu, Z. R.; Wu, J.; Duan, W. H.; Gu, B. L. *Phys. Rev. B* **2008**, *78*, 085423.
(32) Pauling, L. *J. Am. Chem. Soc.* **1932**, *54*, 3570−3582.
(33) Allred, A. L. *J. Inorg. Nucl. Chem* **1961**, *17*, 215−221.
(34) Nakhmanson, S. M.; Calzolari, A.; Meunier, V.; Bernholc, J.; Nardelli, M. B. *Phys. Rev. B* **2003**, *67*, 235406.
(35) Shockley, W.; Queisser, H. J. *J. Appl. Phys.* **1961**, *32*, 510−519.
(36) Zhang, Y. B.; Tang, T. T.; Girit, C.; Hao, Z.; Martin, M. C.; Zettl, A.; Crommie, M. F.; Shen, Y. R.; Wang, F. *Nature* **2009**, *459*, 820−823.
(37) Xia, F. N.; Farmer, D. B.; Lin, Y. M.; Avouris, P. *Nano Lett.* **2010**, *10*, 715−718.